Available online at www.sciencedirect.com
SCIENCE DIRECT
Polymer 47 (2006) 5131–5140
polymer
www.elsevier.com/locate/polymer

Intercalation and viscoelasticity of poly(ether-block-amide) copolymer/montmorillonite nanocomposites: Effect of surfactant

I-Kuan Yang *, Ping-Hung Tsai

Department of Chemical Engineering, Tunghai University, 183 TaichungKang Road, Sec. 3, Taichung, Taiwan, ROC

Received 27 July 2005; received in revised form 24 April 2006; accepted 24 April 2006
Available online 30 May 2006

Abstract

A poly(ether-block-amide) copolymer (PEBA) was successfully hybridized with montmorillonites using melt processing techniques to form nanocomposites. The organoclays used in preparation of the nanocomposites were modified with ammonium surfactants of different molecular structures to study the effect of the surfactant on the intercalation and exfoliation of the polymer by X-ray diffraction (XRD) and dynamic linear viscoelastic analysis. The polymer was found to be capable of forming intercalated composite with unmodified montmorillonite and the best intercalation and exfoliation was found in the hybrids using surfactants that possess hydroxyl group. Organoclays modified with a single tallow tail ammonium prevailed over those modified with a double tallow tail ammonium in intercalation and exfoliation of silicate layers. Higher capacity of ion exchange also led to a better intercalation for hybrids using single tail surfactants, but the hybrids with swallow tail surfactant behaved oppositely. XRD data showed that the diffraction peaks in the hybrids were narrower than those of the organoclay implying a higher order and more number of layers in the stacks of clays. The intercalation of nanocomposites was found dominated by the energetic factor and entropic factor played no role in the outcome of intercalation. Results of linear viscoelastic measurements paralleled those of XRD showing that melts of those nanocomposites with a superior intercalation or exfoliation also exhibited higher storage modulus and thus the linear viscoelasticity could be an indicator for intercalation. The composites showed an abnormal terminal behavior suggesting the existence of a network structure.

Keywords: Poly(ether-block-amide); Nanocomposite; Viscoelasticity

1. Introduction

In the past two decades, polymer/clay nanocomposites attracted a lot of attentions both industrially and academically due to their unique physical properties comparing to neat polymer. The advantages of nanocomposites include enhanced mechanical properties, such as elastic modulus [1] and tensile strength [2,3], improved thermal properties such as coefficient of linear thermal expansion [4], heat distortion temperature [3], flammability resistance [5] and ablation performance [6], and other superiorities in oxygen barrier properties [7,8], water vapor transmission resistance [8] and solvent uptake [9]. Contrast to traditional composites, the physical property enhancements for nanocomposites are achieved with a rather small amount, usually less than 10 vol%, of addition of nanoscale particles. It has been reported that the property enhancement is very much dependent on the morphology and degree of dispersion of the inorganic phase in the polymeric matrix [10].

Clay is generally incompatible with hydrophobic polymers because of its hydrophilic nature. In order to enhance the compatibility between clay and polymers, clays are organically modified by the ion exchange reaction between sodium montmorillonite and ammonium surfactants [11]. The selection of suitable surfactants for clay modification is an important factor for the production of nanocomposites with an excellent exfoliation. Various researchers have studied the effects of the surfactant structure on the preparation of nanocomposites [11–17]. Prior works have shown that surfactant with one long alkyl tail lead to higher levels of organoclay exfoliation than those having two alkyl tails in the case of nanocomposites based on nylon 6 [12,13], poly(methyl methacrylate) [11] and poly(styrene-*co*-acrylonitrile) [14]. For the case of low-density polyethylene [15] and poly (ethylene-*co*-methacrylic acid) ionomer based nanocomposite [16], the effect of the number of alkyl tails shows opposite trend. Moreover, a longer length of alkyl chain of surfactant gives better exfoliation than shorter ones for the clay hybrids with polystyrene [17] and poly(ethylene-*co*-meth-acrylic acid) ionomer [16].

* Corresponding author. Tel.: +886 4 23590262x112; fax: +886 4 23590009.
E-mail address: ikyang@thu.edu.tw (I.-K. Yang).

0032-3861/$ - see front matter © 2006 Elsevier Ltd. All rights reserved.
doi:10.1016/j.polymer.2006.04.065

Polyether-block-polyamide copolymer (PEBA) is a thermoplastic elastomer as well as a segmented copolymer consisting of an aliphatic polyamide as the hard block, a polyether as the soft block and a di-acid serving as the joint between the two blocks. PEBA has been used in a variety of different products, such as antistatic sheets or belts, food packaging materials, virus-proof surgical sheeting or garments, films for textile lamination used in sport wears and gloves, and many others [18]. The polymer in the present study has a trade name of Pebax 3533 that comprises of poly(lauryl lactam) (PA 12) as the hard segment, poly(tetramethylene ether) glycol (PTMO) as the soft segment, and adipic acid as the linkage.

PEBA has been hybridized with inorganic materials to meet the required properties in the application above [19], but it has been rarely reported about the nanocomposites based on this polymer [10]. The preparation of such nanocomposites may be interesting both industrially and academically. As aforementioned the choice of the organoclay or the surfactant that modified the clay should have profound effect on the structure and the properties of the composite formed. To study the effect of surfactant, we prepared PEBA based nanocomposites with seven commercial organoclays that were modified by surfactants of different molecular structures and examined the intercalation and exfoliation of the organoclays and linear viscoelasticity of the composite melts. It was found that structure of the surfactant is crucial to both the intercalation and the viscoelasticity of the hybrids. Energetic factor dominated over the entropy factor in the formation of the nanocomposite. The viscoelasticity and modulus recovery study of the hybrids melts suggested that the clay constructed a network structure by weak connection between platelets and the structure was irrecoverable after large amplitude shearing due to the orientation of the silicate layers. The results of linear viscoelasticity measurements paralleled the results of XRD in intercalation of the polymer and thus the former could be a reliable indicator to the outcome of the intercalation.

2. Experimental

2.1. Materials

The PEBA used in this work was a commercial product of Elf Atochem Inc., Belgium, having a trade name of Pebax 3533. The composition of the segmented block copolymer was determined by ^{1}H NMR spectra to have 36.3 wt% PA 12, 60.1 wt% PTMO, and 3.6 wt% adipic acid. It had an average molecular weight of approximately 50,000 g mol^{-1} [20], and two melting temperatures at 7.6 and 143.9 °C, which are the melting temperatures of PTMO and PA 12, respectively. In the below of text, Pebax 3533 was addressed as P3533. The molecular formula of the polymer can be expressed as:

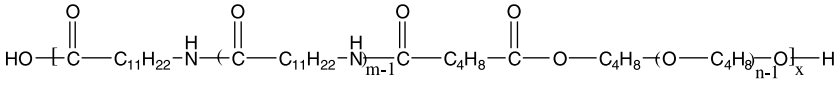

In this study, we employed following seven commercial organoclays: Cloisite 30B, Cloisite 10A, Cloisite 25A, Cloisite 93A, Cloisite 20A, Cloisite 15A and Nanomer I.34TCN and one sodium montmorillonite Cloisite Na$^+$. The first six clays and the sodium montmorillonite were kindly supplied by Southern Clay Inc., USA and Nanomer I.34TCN was supplied by Nanocor Inc., USA. Montmorillonite is a silicate in stacks of limited number of layers. The crystal lattice of montmorillonite consists of two-dimensional layers of about 1 nm thickness. The layers are made of two tetrahedral sheets of silica fused to an edge-shaped octahedral sheet of alumina or magnesia. The lateral dimensions of the layers vary from 70 nm to several microns, which imply that the aspect ratio of the layer could range from 70 to several thousands. Montmorillonite has a chemical formula of $M_x[Al_{4-x}Mg_x]$ $Si_8O_{20}(OH)_4$. M in the formula is a monovalent charge compensating cation. The organoclays were montmorillonites of different ion exchange capacities modified by surfactants of different molecular structures and their physical data were listed in Table 1.

2.2. Sample preparation

Before preparing P3533/clay hybrids, P3533 was placed in a vacuum oven at 80 °C for 24 h to remove moisture, and all organoclays were also treated by the same procedure. Dried polymer was first molten in a blender (Ben Ling Engineering Co. Ltd) at 165 °C, and 86 rpm and then 5 wt% of clay was added and mixed for another 30 min. The resulting product was dried by the same procedure described above and the moisture free sample was then sandwiched between Teflon sheets and heated to 185 °C for about 5 min before thermo-pressed into a film of 1.2 mm thickness at the same temperature. The film was then used in the following characterizations. The hybrids were named after the constituent clays by simply putting a capital P in front of the series numbers of the clays.

2.3. Characterization

XRD characterizations were obtained using a XRD-6000 (Kratos analytical Inc.) equipped with Cu Kα radiation source ($\lambda = 1.54$ Å) operated at 40 KV and 30 mA and the scanning rate was 2 deg/min. Linear viscoelastic properties were measured under nitrogen atmosphere on a rotational type rheometer (RDA II, Rheometrics Co.) using a parallel plate fixture with a gap of 0.8 mm and a diameter of 25 mm. A strain sweep experiment was performed prior to the viscoelastic measurement to ensure that the measurements were within the linear viscoelasticity range. Before collecting any rheological data, thermal stability of P3533 at the testing conditions was checked by monitoring the time period within which the

Table 1
The physical data of the organoclays [21,22]

Type	Surfactant[a]	No. of tails	Modifier conc. (mequiv. /100 g clay)	Nominal d_{001} (Å)[b]
Cloisite Na^+	None	0	92.6	11.7
Cloisite 30B	Methyl, tallow, bis-2-hydroxy ethyl, quaternary ammonium chloride (MT2EtOH)	1	90	18.5
Cloisite 25A	Dimethyl, hydrogenated tallow, 2ethylhexyl quaternary ammonium methyl sulfate(2MHTL8)	1	95	18.6
Cloisite 10A	Dimethyl, benzyl, hydrogenated tallow, quaternary ammonium chloride (2MBHT)	1	125	19.2
Nanomer I.34TCN	Methyl dihydroxy hydrogenated tallow ammonium	2		19.6
Cloisite 93A	Methyl, dihydrogenated tallow, ammonium bisulfate (M2HT)	2	90	23.6
Cloisite 20A	Dimethyl, dihydrogenated tallow, quaternary ammonium chloride (2M2HT)	2	95	24.2
Cloisite 15A	Dimethyl, dihydrogenated tallow, quaternary ammonium chloride (2M2HT)	2	125	31.5

[a] Tallow consisting of ca. 65% C18, ca. 30% C16, and ca. 5% C14.
[b] d_{001} is the gallery height of the layered structure of the montmorrillonites.

modulus G′ and G″ could stay unchanged to ensure that the polymer would remain unharmed by prolonged heating. All rheological measurements were completed within the time limits of thermal stability. All rheological data reported in this work were the average of at least five different measurements.

3. Results and discussion

A brief introduction for the surfactants that modify the montmorillonite will be useful to the discussion. Summarized in Table 1 are the relevant data for the organoclays used in this study. The first one is a Na^+ exchanged montmorillonite with no surfactant modification. The rest of seven organoclays can be divided into two families by the structures of the surfactants. All surfactants used in these organoclays are ammoniums of tallow derivatives. The first family includes Cloisite 30B, 10A, and 25A whose surfactants possess only a single long tallow chain, while the surfactants in the second family including Nanomer I.34TCN, Cloisite 93A, 20A and 15A possess tail of two tallow chains, or a swallowtail. The number of tallow chains, or tails, has a profound effect on the properties of the nanocomposites as will be shown below. Cloisite 30B and Nanomer I.34TCN enjoy a unique feature that their surfactant molecules possess pendent hydroxyl groups, which bring them the excellence in either intercalation or viscoelasticity. Ion exchange capacity and nominal d_{001} spacing of organo-clays are also shown in the table, but the values of the latter are slightly different from our XRD measurements.

Fig. 1 shows the XRD patterns for sodium montmorillonite and seven organoclays. All clays show an identifiable broad first order diffraction peak with a very small second order peak and third order peak is not detectable. The peak position can be translated into the peak d_{001} spacing or d-spacing of the clays by Bragg's law ($n\lambda = 2d \sin\theta$). The results are summarized in Table 2. The sodium montmorillonite has the smallest peak d-spacing, which is reasonable since no surfactant fills in the galleries between the silicate platelets. The clays modified by surfactants with a single alkyl tail have a smaller peak d-spacing than those modified by swallow tail surfactants, though the former has a broader distribution of the interlayer distance than the latter does as manifested by their broader peaks in Fig. 1. That the swallow tail modified clays has a larger d-spacing can be interpreted by the followings: Tallow consists of hydrocarbon chains with the number of carbon atoms ranging from 16 to 18. The apolar surfactant chains residing in the galleries of the clays radiate away from the polar silicate surface and adopt more extended conformations. With the same amount of ammonium exchanged, the spacing between the cationic head groups of the ammoniums is the same and in order to accommodate twice amount of the apolar chains the molecules of the swallow tail surfactants have to adopt a more extended conformation and hence greater gallery

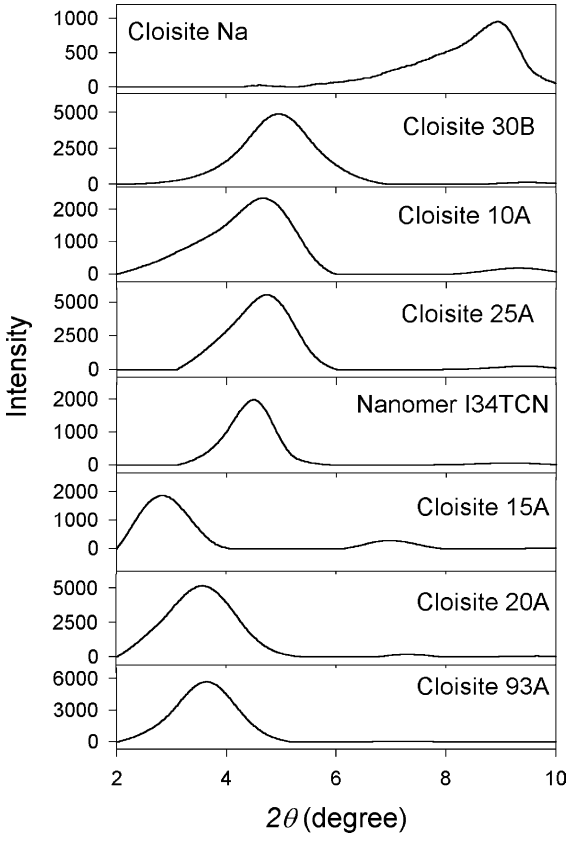

Fig. 1. The XRD patterns of clays.

Table 2
The results of *d*-spacing and increment in d-spacing upon hybridization

Hybrids	Clay			Hybrid			Gain in *d*-spacing (Å)
	2θ	d_{001} (Å)	N^*	2θ	D_{001} (Å)	N^*	
PNa	8.94	9.88	5.5	4.88	18.1	–	8.22
P30B	4.94	17.9	3.2	2.28	38.7	–	20.8
P10A	4.68	18.9	3.1	2.62	33.7	5.6	14.8
P25A	4.72	18.7	3.4	2.82	31.3	7.8	12.6
PI34	4.50	19.6	4.5	2.28	38.7	–	19.1
P20A	3.56	24.8	2.4	2.44	36.2	4.7	11.4
P93A	3.64	24.2	2.7	2.76	32.0	3.7	7.80
P15A	2.82	31.3	2.5	2.28	38.7	5.8	7.40

N^*, average number of layer in each stack.

heights result. The thickness of a silicate layer of the montmorillonite is 9.5 Å [23] and gallery heights of the organoclays can be determined by the differences between *d*-spacing and the layer thickness. Excluding Nanomer I.34TCN the gallery heights of the organoclays in the swallowtail family are in the range of 12.5–14.7 Å which is about a half of a fully stretched chain length of an octadecyl carbon chain, it is speculated that the tallow tails in the galleries adopt a nearly fully extended conformation, which is tilted to the silicate surface [24]. Higher ionic exchange capacity leads to larger *d*-spacing for both families, which is reasonable since more exchanged surfactant molecules bring more crowdedness and hence higher *d*-spacing. There are at least three reasons for the broadening of the peak: instrumental effects, limited size or limited number of layers in the stacks of organoclays and imperfect order in the layer arrangement. The broadening of the diffraction peaks could imply that the organoclays and the sodium montmorillonite have a less ordered stack of layered structure and a less average number of layers in each stack of organoclay, which represents a broad distribution of the d_{001} spacing. To estimate the average number of layers in each stack of the clays by consideration of both factors, i.e. the limited size and the imperfect order would be too complicated. The effect of limited size can be represented by Scherrer equation. Using Scherrer equation to estimate the size of the stack gives the lower bound of the average number of layers per stack since the instrumental and imperfect order effect are neglected. The average number of layers per stack for each organoclay is listed on Table 2 and they range from 2.4 to 4.5.

It is noted that the clays modified by surfactants possessing hydroxyl groups, Cloisite 30B and Nanomer I.34TCN, have the smallest peak *d*-spacing among their family members. The polar hydroxyl groups offer surfactant chains the affinity to the silicate surface such that the surfactant chains counteract the expelling force between the hydrocarbon segments and the silicate surface. Consequently, the tallow tails could assume a more disorder and lateral conformation and result in a smaller peak *d*-spacing.

Shown in Fig. 2 are the XRD spectra of eight different hybrids and the pristine polymer Pebax 3533. The XRD spectrum of the polymer shows a weak and broad peak covering a range of 2θ from 3.5 to 7.0°. The XRD spectra of the eight hybrids show multiple diffraction peaks but the higher order diffraction peaks merge into the peak of the matrix polymer and becomes difficult to identify. The first order diffraction peak of hybrid PNa is small and nearly combines with the broad peak from the polymer. For hybrids using surfactant with hydroxyl groups, i.e. P30B and PI34 the first order peak is hardly identifiable indicating that the clay is almost completely exfoliated. The intensities of the peak for the hybrids modified by single tail surfactants are also negligibly small and in fact they are smaller than the intensity of the polymer diffraction peak. The low intensities of the peaks essentially indicate that the number of the ordered diffraction centers is relatively low and there may be a considerable amount of single layer silicate or equivalently a high extent of exfoliation in these hybrids. In contrast to hybrids of the single tail family, both the first and second order diffraction peaks of the hybrids of swallow family such as P15A, P20A and P93A are relatively sharper and more intense though the hybrid PI34 which uses hydroxyl surfactant is an

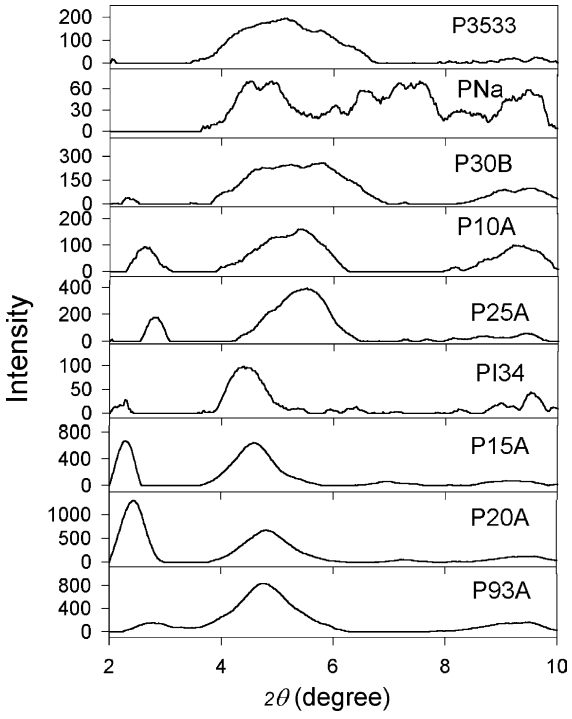

Fig. 2. The XRD patterns of hybrids and neat P3533.

exception in the swallow tail family and it has a weak and broad first order peak similar to those of the hybrids with single tail surfactants. It is worthwhile to examine the diffraction patterns of the swallow tail hybrid family in details. The diffraction pattern of P20A resembles to that from crystal, namely the first order peak is sharper and higher than the second order peak. While for P15A, the second order peak, though broader, is of nearly the same height as the first order. The diffraction pattern of P93A is unusual since the first order peak is smaller than the second order peak. It is reasonable that when overlapping with the broad peak of the diffraction from polymer matrix, the second order peaks of swallow tail hybrid family should become higher than an ordinary one, but such overlapping cannot make the second order peak higher than the first order one. We speculate that the apparent second order peak from P93A is in fact a combination of the second order peak relating to the first order peak at $2\theta = 2.76^\circ$ and another first order peak from stacks of ordered silicate layers of smaller *d*-spacing. This implies that the silicate layers in P93A partition into two groups, which exhibit two different sets of peaks. The partition of the silicate layers may also happen to P15A since the first and second order peak of this hybrid are nearly of the same height. The partition of silicate layers is theoretically possible, which could be a coexistence of two phases [25].

The sharp and intense first order peaks in the swallow tail hybrid family reveal that in comparison with the single tail hybrid family, with the exception of PI34, the number of diffraction centers in this hybrid family is higher and the stacks of silicate layers are more ordered. Consequently, it is reasonable to claim that the isolated silicate layers in these hybrids are fewer, or the extent of the exfoliation is less. The partition of the silicate layers in P93A and P15A could make the extent of exfoliation worse and consequently the extent of exfoliation for P93A, P20Aand P15A should follow the sequence of P20A > P15A > P93A. As shown in Table 1 that Cloisite 20A and 15A use the same surfactant for modification but their ion exchange capacities are not equal, while Cloisite 93A has a different surfactant and a ionic capacity slightly lower than that of 20A. The subtle difference in the surfactant and ionic exchange capacity may be responsible for the different extent of exfoliation in the corresponding hybrid.

The gain in the *d*-spacing after hybridization may be also an indicator of the extent of exfoliation. The positions of the first order peaks were translated into the peak *d*-spacing values and summarized in Table 2 together with the gain in the *d*-spacing after hybridization. From this table, the following observations were noted: (i) the *d*-spacing of the clay layered structure in the composite using sodium montmorillonite, i.e. PNa, is enhanced, which means the polymer molecules are able to penetrate into galleries between the hydrophilic silicate surfaces and reside in there. (ii) There exist stacks of layered silicate within all composites though the amount of the stacks may be small in the hybrids of the single tail family. The *d*-spacing of the hybrids, or the gallery height between the silicate platelets, ranged from 31.3 to 38.7 Å after hybridization. Though there was only slight difference in the *d*-spacings of the hybrids, the gains in *d*-spacing for clay/polymer hybrids had a great difference and they can be arranged in the sequence of P30B > PI34 > P10A > P25A > P20A > PNa > P93A > P15A.

To realize intercalation of a polymer into the gallery of clay, the energy released must compensate the entropy loss upon hybridization as described by the following inequality.

$$\Delta G = \Delta H - T\Delta S < 0 \quad (1)$$

The enthalpy change ΔH summarizes the interaction between members of the constituent pair such as polymer and surfactant, polymer and silicate surface, surfactant and silicate surface, while the entropy change ΔS results from the gain in releasing the constraint to the surfactant chains upset by the loss in confinement of the polymer molecules upon hybridization. The intercalation of the polymer into the sodium montmorillonite manifests that there must be a favorable interaction between polymer molecules and the unmodified silicate surfaces such that a considerable amount of energy was released to compensate the entropy penalty of the confinement of the polymer molecules in the galleries. The interaction between the polymer molecules and the silicate surface may originate from the hydrophilic nature of both the PTMO and PA12 segment.

Three important results can be extracted from the sequence of gain in gallery height. First, organoclays with a single tallow tail obtains a greater gallery expansion than those organoclays with a swallowtail do with an exception of PI34. Second, in the family of single tail surfactant, increasing ion exchange capacity increases the gallery expansion as demonstrated by P25A and P10A, while in the family of swallow tail surfactant the opposite trend is observed. Third, the hybrids in the leading positions of the sequence have hydroxyl moiety in the surfactant used.

The swallowtail surfactants were demonstrated disadvantageous to the accommodation of the polymer molecules in gallery in this PEBA/montmorillonite system. Similar results were reported for clay hybrids of polar polymers such as poly(methyl methacrylate) [11], nylon 6 [12,13], and poly(-styrene-*co*-acrylonitrile) [14], but opposite results were also reported for those of apolar polymers like low density polyethylene [15] and poly (ethylene-*co*-methacrylic acid) ionomer [16], and less polar polymer like polystyrene [26]. The inconsistency in the results is not well interpreted so far, but the polarity difference in the polymers of opposite behavior seems to provide the answer. Giannellis et al. demonstrated both theoretically and experimentally in a series of studies [26,27] that the entropy gained associated with the surfactant layer separation was unable to balance the entropy loss associated with the confinement of a polymer melt and consequently the entropy penalty to the confined polymer is not prohibitive to hybrid formation and the outcome of the hybrid formation was dominated by the energetic factors which included the pair interactions of silicate surface/polymer, silicate surface/surfactant and surfactant/polymer as mentioned above. The intercalating behavior of the hybrid system of our polymer and organoclays is strictly dominated by the energetic factor.

The affinity between the poly(ether-block-amide) and the silicate surface has been evidenced by the intercalation of the polymer into the unmodified sodium montmorillonite. Our system parallels the nylon 6 nanocomposite [12,13]. The noticeable interaction between the polymer and silicate surface plays an important role in the outcome of the hybridization and thus the access of the polymer segment to the silicate surface and surfactant is crucial to the formation of nanocomposites. Thermodynamically, the apolar tallow tail tends to reject the polar polymer segments and increasing number of the apolar tallow tail deprives of the opportunity of the polar polymer segments in getting the access to the silicate surface by sterically blocking the surface [12]. On the contrary for composites that use apolar or less polar polymers, the interaction between the apolar surfactant tail and the polymer molecules becomes an advantage to the intercalation and hence higher tallow chain density is beneficial to the intercalation of apolar polymers and behavior opposite to those of polar polymers is thus observed. The opposite trend shown by the swallow tail surfactant family in the effect of ion exchange capacity on the intercalation can also be explained by the expulsion of the polymer molecules by the surfactant tail. Higher ion exchange capacity translates into more expulsive tallow tails that expel and block the access of the polar polymer segments to the silicate surface.

That higher ion exchange capacity leads to better intercalation in the single tail surfactant family can be explained by the interaction between the polymer and the ammonium head. Higher ion exchange capacity translates into a larger number of ammonium heads per unit silicate surface area, which interact with the polar polymer molecules and contribute a more negative enthalpy change upon hybridization resulting in the promotion of intercalation and exfoliation.

For the two leading hybrids in the sequence, the surfactant molecules that modify the two clays have two hydroxyl groups. The leading position in expansion of *d*-spacing for P30B and PI34 is the results of twofold beneficial energetic interactions. In addition to the interaction between the polymer and the silicate surface, these two surfactants enjoy an additional advantage of polymer-surfactant interaction. The hydroxyl group in the surfactants is able to form hydrogen bonding with both the hard and soft segment of the polymer, which contributes a favorable enthalpy change upon hybridization.

The average number of layers per stack was also estimated and summarized in Table 2. Interestingly, the average number of layers increases after hybridization. At first glance, one feels that it is conflicting that hybridization enhances the *d*-spacing of the organoclays and to some extent splits the organoclays to allow the presence of isolate platelets and simultaneously, increases the number of layers in stacks. To accommodate the 'conflicting' observations from the diffraction, we propose a model in Fig. 3 which is realized by the large aspect ratio of the montmorillonite platelets. Because of the large aspect ratio, platelets of montmorillonite are in fact flexible and this is well demonstrated in the transmission electron microscopic pictures of nanocomposites of this kind [28–30]. As seen in the figure, the isolated platelets formed upon hybridization could register

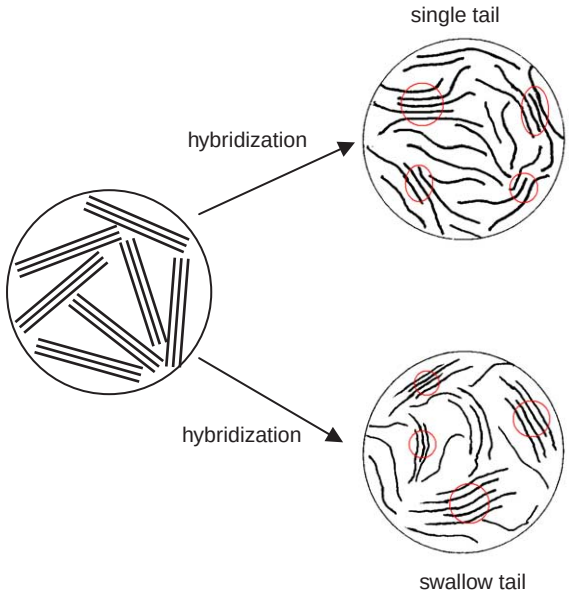

Fig. 3. The proposed model for the stacks of the silicate layers. Note that for single tail family there is only stacks of one *d*-spacing, while for swallow tail family there are stacks of two different *d*-spacings reflecting the unusual ratio of the height of the first order peak to that of second order peak.

a segment of them with segments of other platelets to form ordered diffraction centers (the encircled regions). The diffraction centers could possibly play the role of cross-linking site, which eventually leads to the formation of network. In this way, the diffraction centers can have an enhanced *d*-spacing in company with larger number registered layers. The situation for swallow tail hybrids is slightly different from that of single tail hybrids. Due to the low extent of exfoliation, the former has less number of isolated platelets and there are stacks of different *d*-spacing to represent two sets of diffraction peaks mentioned above.

Fig. 4 shows that the strain dependence of the shear moduli of the hybrids and neat P3533 at 170 °C and 1 rad/s. The following observations were found from the figure: (i) Putting aside the hybrid PNa, the hybrid melts have dynamic shear moduli higher than those of the neat P3533, and the values of both shear moduli of the hybrid melts follows the sequence P30B ≒ PI34 ≒ P10A > P25A > P20A > P15A > P93A > PNa ≒ P3533 which almost completely repeats the sequence of intercalation aforementioned and the only difference is the position switching of P15A and P93A. Additionally, there are three orders of magnitude difference between the highest and lowest storage moduli in this sequence. (ii) The melt of the neat polymer has an extremely wide range of linear viscoelastic window, which is more than several hundred percents of strain. The shear moduli of the melt of PNa almost completely duplicate those of the polymer melt. For the rest of the hybrids their melts have a much smaller linear viscoelastic window, and a strain weakening in dynamic shear modulus occurs when the strain applied exceeds a critical value.

Fig. 5 shows the linear viscoelastic spectra of the hybrids and neat P3533 at 170 °C. Melt of P3533 behaves exactly like a normal polymer: the terminal slope, or the slope at very low

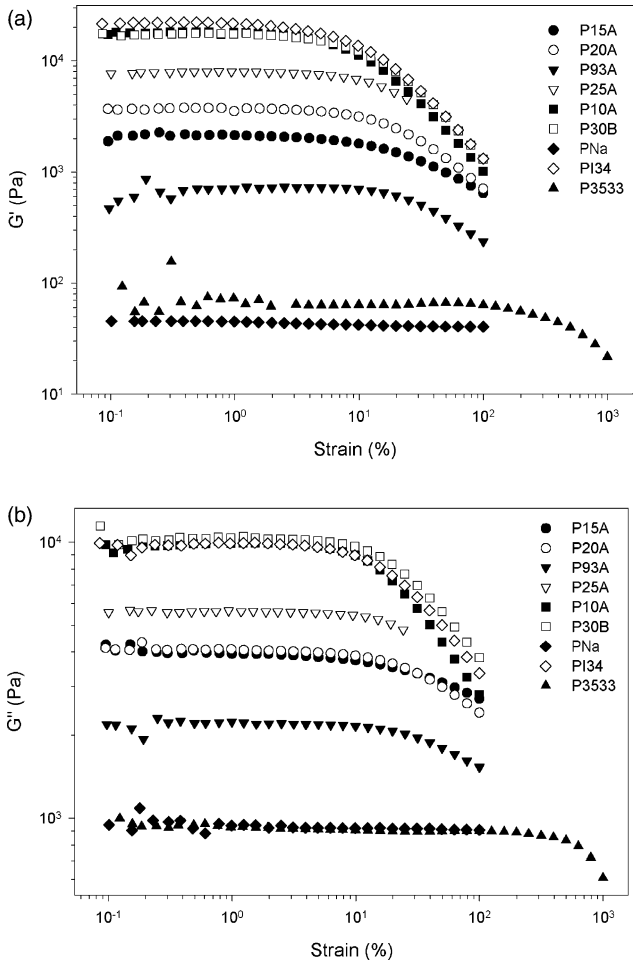

Fig. 4. The strain sweep of hybrids and neat P3533 at 170 °C, 1 rad/s. (a) G′ and (b) G″.

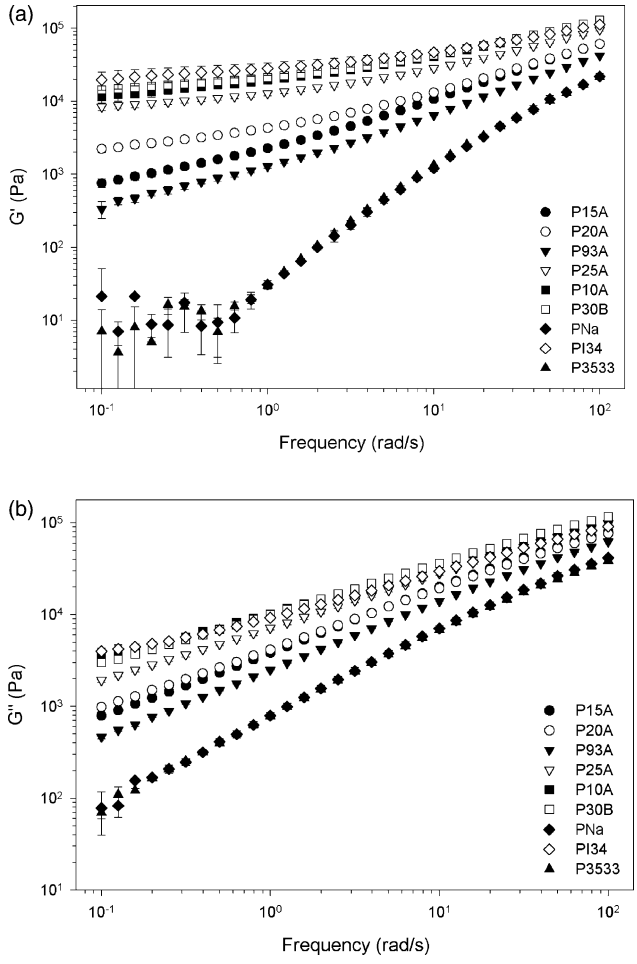

Fig. 5. The dynamic mechanical spectra of hybrids and neat P3533 at 170 °C. (a) G′ and (b) G″.

frequencies, of G″ is equal to 2 and for G′ the terminal slope is very close to 1 as a normal polymer melt does until a plateau emerges at frequency of 0.8 rad/s demonstrating the unique characteristic of this block copolymer [31]. At all frequencies investigated, the storage and loss modulus of PNa are nearly the same as those of neat polymer. Apparently in this hybrid, the intercalation the polymer molecules into the clay galleries has no contribution to the viscoelasticity of the melts. The composite exhibits the same as those conventional composites do. The melts of PI34 and hybrids of the single tail family can be lumped into one category by their similarity in viscoelastic behavior. These melts exhibit an abnormal terminal behavior which is described by a plateau at about 10^4 Pa of G′ at low frequencies and by slightly smaller value of G″ with a terminal slope deviating from 2. Among these melts, melts of PI34 and P30B have the highest storage and loss moduli as well as the smallest terminal slopes, followings are melts of P10A and P25A in sequence. In contrast to the single tail family, the members in the swallow family show considerable differences in their moduli especially in the low frequency region. Over the frequencies investigated, the value of either storage and loss modulus follows the sequence: PI34 ≒ P30B > P10A > P25A > P20A > P15A > P93A > PNa ≒ P3533. Overall speaking, hybrids with higher extent of exfoliation such as P30B, PI34 and P10A, have a stiffer structure, which demonstrates higher dynamic moduli and narrower linear viscoelastic windows and contrarily the less exfoliated hybrids show a somewhat softer structure and inferior moduli.

The coincidence of the shear modulus sequence with the intercalation sequence could not simply be accidental. The shear moduli were measured at higher temperatures and in molten state while XRD spectra were obtained at room temperature and in solid state. The coincidence suggests that when the melts are subject to a solidification process the solid outcome of the process still faithfully preserve the characteristics of the melts, especially the organization of the platelets in molten state such that higher viscoelastic moduli in molten state can be translated into better intercalation and exfoliation observed from the X-ray diffraction. Similarly, after melting, the melts preserve the state of intercalation and exfoliation in the solid state. This is expected. Firstly, the polymer matrix is so viscous that each silicate layer has very slim chance to get combined with the others in the cooling or melting process. Secondly, the radius of gyration for a polymer molecule in the solid state is nearly the same as that in the molten state no matter the polymer is crystalline or amorphous [32] and the

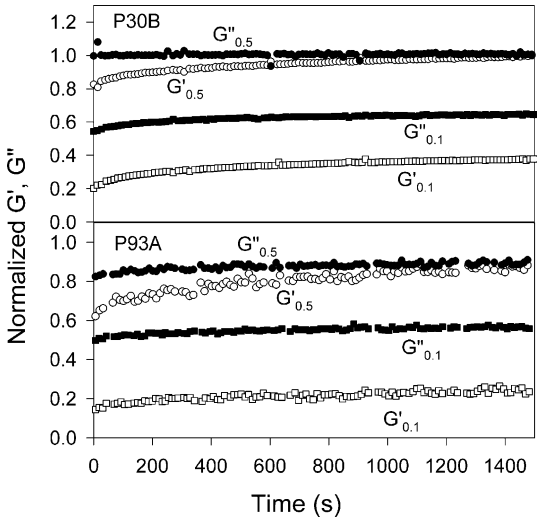

Fig. 6. The recovery of G′ and G″ after cessation of large amplitude oscillatory shear. The pre-shearing and the recovery process proceeded at 170 °C and the monitoring of the moduli was performed at the same temperature and 1 rad/s.

conservation of polymer molecule dimension prevents the combination of the platelets of clays and hence the state of intercalation and exfoliation is preserved. Naturally, the linear viscoelasticity could be an indicator of intercalation and exfoliation.

To get better understanding of the structure, we pre-sheared the hybrid melts at strain amplitudes that were high enough to cause strain weakening and monitored the recovering process of both G′ and G″. Shown in Fig. 6 are the evolutions of shear muduli after large amplitude oscillatory shear. The melts of hybrids P30B and P93A, were pre-sheared to an amplitude at which the storage modulus was a half or one tenth of the storage modulus value in the linear viscoelastic window before the recovery of G′ and G″ was allowed and monitored. The corresponding strain amplitudes for this test were 20 and 100% for P30B and 80 and 300% for P93A, respectively. Either modulus is normalized by its respective modulus in the linear viscoelastic window. For convenience, we will call the normalized moduli recovering from the half storage modulus pre-shear $G'_{0.5}$ and $G''_{0.5}$ and those moduli recovering from the one-tenth storage modulus pre-shear $G'_{0.1}$ and $G''_{0.1}$. It was found that for melts of both hybrids, their storage moduli, either $G'_{0.5}$ or $G'_{0.1}$, experience a rapid recovery followed by a sluggish growth; after cessation of the pre-shear, $G'_{0.5}$ of P30B melt, which is a hybrid with a higher extent of exfoliation, immediately grows from 50 to 80% and a complete recovery is obtained, signifying the full restoration of the structure, when the elapsed time is about 1200 s. As for melt of P93A, a hybrid of a lower extent of exfoliation, $G'_{0.5}$ experiences an immediate growth from 50 to 60% before a sluggish recovery to 80% of its linear viscoelastic value at elapsed time of 1400 s. The high percentage of recovery in G′ reveals that the pre-shear strain amplitude, 20 and 80% for P30B and P93A, respectively, is not large enough to destroy the structure. Similar behavior is found for $G'_{0.5}$s of the two hybrids but with a much inferior recovery indicating the destruction of the structure by pre-shearing at amplitude of 100 and 300%, respectively, for the melts. The recovery of loss moduli is faster than that of storage moduli. In fact, the recovery of $G''_{0.5}$s for both melts are almost instantaneous, indicating that the dissipation of the melts is dominated by the polymer matrix since it has a much small relaxation time than structure associated with platelets of clays. Another evidence for the dominant role of the matrix in dissipation is that the value that for P30B $G''_{0.1}$s recovered is very close to that of the matrix.

The solid like behavior at terminal frequencies has been attributed to the solidification of the melt or liquid in confinements [33–35], the formation of the three-dimensional network [36,37], or simply to the physical jamming of the dispersed platelets. The solidification of the melt occurs when molecules of liquids or polymer melts are confined in an environment of dimension of about fivefold of the radius of gyration or R_g of the molecule [35]. Our XRD results revealed that the intercalation of PEBA molecules into the galleries of the naked montmorillonite does occur with a *d*-spacing of 18.1 Å which means that the polymer molecules are confined in galleries in height of 9.1 Å, since the thickness of the silicate layer is about 9 Å. The polymer used in this study has a molecular weight of 50,000, which corresponds to a unperturbed R_g of 70 Å for the molecule. The dimension of the confinement in this study is comparatively smaller and in fact the dimension is smaller than the dimension of 'hard wall' below which the repulsive force becomes infinite and the confinement cannot be achieved [33]. One possible interpretation for the intercalation in PNA hybrid is that only segments or ends of the polymer molecules penetrate into the galleries and the interaction between the silicate surface and the molecule segments is so weak that no solidification actually occurs and the viscoelasticity of the hybrid does not deviate from that of the neat polymer. The *d*-spacing for the rest of hybrids ranges from 31.3 to 38.7 Å, which corresponds to a gallery height from 21.8 to 29.2 Å. The dimension of the gallery height is about one half of the R_g of the polymer molecule and the space that is available for the accommodation of the polymer molecules should be smaller when the competition of the surfactants for the space is taken into account. The solidification was reported as a glass like transition with diminishing dimension of the confinement and at about fivefold of the unperturbed R_g of the polymer molecule [35] and hence solidification of the confined polymer molecules could happen. There is also the possibility that the isolated platelets could form confinements of larger dimensions, which can be estimated from the volume fraction of the silicate layers. The weight fraction of the organoclays for the hybrids is 5%. From the densities of the montmorillonite, the polymer and the surfactant the volume fractions of the silicate layers are estimated to be 1.5%, which is consistent with our thermogravimetric analysis. If the silicate layers are completely exfoliated as in the hybrids of PI34 and P30B, the average distance between two isolated platelets is estimated as 67 nm, by the assumption of the parallelism between the platelets. Israelachvili et al. reported that for polybutadienes the deviation of the viscoelastic moduli from those in the bulk

of the melt started to grow exponentially when the confinement dimension was below 10 times the R_g of the polymer molecule [38]. The ratio of the average distance estimated above to the R_g of the polymer molecule in the exfoliated hybrids in this study is amount to 10, indicating that the solidification possibly occurs between the isolated platelets. Though the solidification may possibly occur in both ordered stacks and between isolated platelets, the incomplete recovery of the structure after large amplitude pre-shear cannot be explained simply by solidification from confinement unless the solidification provides anisotropy in viscoelasticity.

Network of card-house structure has been proposed in polypropylene/clay nanocomposites [30] and in aqueous montmorillonite suspensions [40–42]. Card-House structure is essentially built on the edge-face contact in clay platelets. In aqueous suspensions, the long-range coulombic force is responsible for the contact, while for suspension in a polymer matrix, bridging by the polymer molecules could replace the role of coulombic force in aqueous systems. The abnormal terminal behavior could be explained by the three-dimensional network and the incomplete recovery after pre-shear can be simply resorted to the destruction of the network and orientation of the platelets [39] which had been verified by various techniques including scattering measurements, electron microscopy, and linear viscoelastic measurements in dynamic shear field [36]. End-tethered nanocomposites [43] which bridge silicate layers by strong adsorption of polymer molecules showed strain hardening due to the stretching of the molecules. Contrarily the hybrids in this study show strain-weakening implying that the bridging by the polymer molecules is a weak interaction. The high storage modulus and the small terminal slope exhibited by melts of the hybrids of the single tail family could be attributed to more extent of exfoliation and hence more contacts between platelets. The immediate growth in storage modulus after the pre-shear can be referred to the restoration of contacts by the polymer molecules in the vicinity since the links were polar group interactions. Obviously, the faster recovery of P30B over P93A immediately after the cessation of pre-shear indicates that the surface of the silicate layer in the former has more affinity to the polymer molecules. The sluggish growth and the failure in complete recovery of $G'_{0.1}$ and $G''_{0.1}$ should be the results of the shear alignment of the silicate layers since the un-oriented state of the layers before pre-shear is very difficult to recover after shear alignment due to the high viscosity of the melts. While using the network to explain the rheological behavior of the hybrid melts, one cannot deny that the physical jamming can contribute high values of both viscoelastic moduli. Liquid crystals are known to have a higher viscosity at un-orientated or isotropic state than at oriented or liquid crystalline state [44,45]. Based on the excluded volume effect, the critical volume concentration for the formation of liquid crystalline phase is of the order of the aspect ratio of the suspending particles. By the aspect ratio of the silicate layer one can obtain the critical concentration for the silicate layer suspension as 1.5%, which is exactly the volume concentration of the hybrids in this study. Thus, the un-oriented state before pre-shearing could be a un-equilibrium state and the oriented state could be the state at equilibrium. Nevertheless, other forces involving in the formation of the nanocomposite could complicate the rheological and the phase transition behavior which needs more elaborated work.

4. Conclusion

Segmented polymer Pebax 3533 was successfully hybridized with eight different clays to form a series of nanocomposites. XRD diffraction and rheological characterization were performed to investigate the effect of the surfactants that modified the clays on the properties of the hybrids. The XRD results showed that the hybrids constituted of the organoclay modified by the surfactant with a single long alkyl tail had a higher extent of exfoliation than those prepared by the organoclay modified by the surfactant with a swallow tail. Hydroxyl groups in the surfactant modifying clays enhanced the interaction with the polymer matrix resulting in a higher extent of exfoliation of clays. Energetic factor was found to dominate over the entropy factor in the formation of the nanocomposites. The rheological results paralleled those of XRD and faithfully reflected the extent of exfoliation and the structure of hybrid by linear viscoelasticity: a higher extent of exfoliation translated into a higher shear modulus, a smaller linear viscoelastic window and a faster and better structure recovery. Both the extent of exfoliation and the orientation of the silicate layers affected the modulus of the hybrid melts. The abnormal terminal behavior exhibited by the melts of the hybrids could be the results of network structure. Linear viscoelasticity could be an indicator for the examination of the extent of exfoliation for hybrid prepared.

Acknowledgements

The authors wish to thank the National Science Council of the Republic of China for the financial support under the contract no NSC 93-2216-E-029-002- to this research.

References

[1] Osman MA, Rupp JEP, Suter UW. Polymer 2005;46(5):1653–60.
[2] Song M, Wong CW, Jin J, Ansarifar A, Zhang ZY, Richardson M. Polym Int 2005;54(3):560–8.
[3] Shishan W, Dingjun J, Xiaodong O, Fen W, Jian S. Polym Eng Sci 2004; 44(11):2070–4.
[4] Yoon PJ, Fornes TD, Paul DR. Polymer 2002;43(25):6727–41.
[5] Chen-Yang YW, Yang HC, Li GJ, Li YK. J Polym Res 2004;11(4): 275–83.
[6] Vaia RA, Price G, Ruth PN, Nguyen HT. Lichtenhan J Appl Clay Sci 1999;15(1–2):67–92.
[7] Krook M, Morgan G, Hedenqvist MS. Polym Eng Sci 2004;45(1):135–41.
[8] Osman MA, Mittal V, Morbidelli M, Suter UW. Macromolecules 2004; 37(19):7250–7.
[9] Pramanik M, Acharya H, Srivastava SK. Macromol Mater Eng 2004; 289(6):562–7.
[10] Majumdar D, Dontula N, Blanton TN, Freedman GS., EP Patent Number 1312582, 2003 (assignee to Eastman Kodak Company, US).
[11] Kumar S, Jog JP, Natarajan U. J Appl Polym Sci 2003;89(5):1186–94.
[12] Fornes TD, Hunter DL, Paul DR. Macromolecules 2004;37(5):1793–8.

[13] Fornes TD, Yoon PJ, Hunter DL, Keskkula H, Paul DR. Polymer 2002; 43(22):5915–33.
[14] Stretz HA, Paul DR, Li R, Keskkula H, Cassidy PE. Polymer 2005;46(8): 2621–37.
[15] Hotta S, Paul DR. Polymer 2004;45(22):7639–54.
[16] Shah RK, Hunter DL, Paul DR. Polymer 2005;46(8):2646–62.
[17] Xie W, Hwu JM, Jiang GJ, Buthelezi TM, Pan WP. Polym Eng Sci 2003; 43(1):214–22.
[18] Information available from the website of Elf Atochem Inc. (http://www.atofina.com).
[19] Feller JF, Langevin D, Marais S. Synth Met 2004;144(1):81–8.
[20] Bondar VI, Freeman BD, Pinnau I. J Polym Sci, Polym Phys 1999;37(17): 2463–75.
[21] Physical properties bulletin from Southern Clay Products, Inc. (http://www.nanoclay.com/).
[22] Taft KM, Kurano MR, Mada KAN., US Patent Number 20040048129, 2004 (assignee to Hoku Scientific, Inc., Honolulu, HI, US).
[23] Brindley GW, Brown G, editors. Crystal structures of clay minerals and their X-ray identification. London: Mineralogical Society; 1980.
[24] Vaia RA, Teukolsky RK, Giannelis EP. Chem Mater 1994;6(7):1017–22.
[25] Vaia RA, Liu WD, Koerner H. J Polym Sci, Polym Phys 2003;41(18): 3214–36.
[26] Vaia RA, Giannelis EP. Macromolecules 1997;30(25):8000–9.
[27] Vaia RA, Giannelis EP. Macromolecules 1997;30(25):7990–9.
[28] Krishnamoorti R, Vaia RA, Giannelis EP. Chem Mater 1996;8(8): 1728–34.
[29] Gelfer M, Song HH, Liu L, Avila-orta C, Yang L, Si M, et al. Poly Eng Sci 2002;42(9):1841–51.
[30] Okamoto M, Nam PH, Maiti P, Kotaka T, Hasegawa N, Usuki A. Nano Lett 2001;1(6):295–8.
[31] Yang IK, Tsai PH. J Polym Sci, Polym Phys 2005;43(17):2557–67.
[32] Gedde UW. 1st ed Polymer physics. London: Chapman and Hall; 1995 [chapter 2].
[33] Demirel AL, Granicks S. J Chem Phys 2001;115(3): 1498–512.
[34] Granick S. Phys Today 1999;July:26–31.
[35] Hu HW, Granicks S. Science 1992;258:1339–42.
[36] Krishnamoorti R, Yurekli K. Curr Opin Colloid Interf Sci 2001;6(5–6): 464–70.
[37] Mishra JK, Hwang KJ, Ha CS. Polymer 2005;46(6):1995–2002.
[38] Luengo G, Dchmitt FJ, Hill R, Israelachvili J. Macromolecules 1997; 30(8):2482–94.
[39] Krishnamoorti R, Ren JX, Silva AS. J Chem Phys 2001;114(11): 4968–73.
[40] Heath D, Tadros TF. J Colloid Interf Sci 1983;93(1):307.
[41] Brandenburg U, Lagaly G. Appl Clay Sci 1998;3(2):263.
[42] Sohm R, Tadros TF. J Colloid Interf Sci 1989;132(1):62.
[43] Giannelis EP, Krishnamoorti R, Mania E. Adv Polym Sci 1999;138: 108–47.
[44] deGenne G, Prost J. 2nd ed The physics of liquid crystals. New York: Oxford Science; 1993 [chapter 2].
[45] Doi M, Edwards SF. 1st ed The theory of polymer dynamics. NewYork: Oxford Science; 1988 [chapter 9].